

Earth and Space Science



RESEARCH ARTICLE

10.1029/2021EA002010

Key Points:

- Precipitation extreme (PE) responds to a large global warming range, for example, from 0 to 5 K, in a nonlinear fashion
- Cautions in using single forcing simulations to quantify the PE response to greenhouse gas (GHG) and aerosols, due to the nonlinearity
- PE response to aerosols is stronger than to GHG, but the difference is smaller than previously estimated

Correspondence to:

Y. Xu,
yangyang.xu@tamu.edu

Citation:

Xu, Y., Lin, L., Diao, C., Wang, Z., Bates, S., & Arblaster, J. (2022). The response of precipitation extremes to the twentieth- and twenty-first-century global temperature change in a comprehensive suite of CESM1 large ensemble simulation: Revisiting the role of forcing agents vs. the role of forcing magnitudes. *Earth and Space Science*, 9, e2021EA002010. <https://doi.org/10.1029/2021EA002010>

Received 13 SEP 2021
Accepted 12 DEC 2021

Author Contributions:

Conceptualization: Yangyang Xu, Lei Lin

Formal analysis: Lei Lin, Chenrui Diao

Methodology: Yangyang Xu, Lei Lin, Susan Bates, Julie Arblaster

Resources: Susan Bates

Software: Julie Arblaster

Supervision: Yangyang Xu

Validation: Chenrui Diao, Julie Arblaster

Writing – original draft: Yangyang Xu, Lei Lin

© 2021 The Authors. Earth and Space Science published by Wiley Periodicals LLC on behalf of American Geophysical Union.

This is an open access article under the terms of the [Creative Commons Attribution-NonCommercial-NoDerivs License](https://creativecommons.org/licenses/by/4.0/), which permits use and distribution in any medium, provided the original work is properly cited, the use is non-commercial and no modifications or adaptations are made.

The Response of Precipitation Extremes to the Twentieth- and Twenty-First-Century Global Temperature Change in a Comprehensive Suite of CESM1 Large Ensemble Simulation: Revisiting the Role of Forcing Agents Vs. the Role of Forcing Magnitudes

Yangyang Xu¹ , Lei Lin² , Chenrui Diao¹ , Zhili Wang³, Susan Bates⁴, and Julie Arblaster^{4,5} 

¹Department of Atmospheric Sciences, Texas A&M University, College Station, TX, USA, ²School of Atmospheric Sciences, Sun Yat-sen University, Zhuhai, China, ³State Key Laboratory of Severe Weather and Key Laboratory of Atmospheric Chemistry of CMA, Chinese Academy of Meteorological Sciences, Beijing, China, ⁴National Center for Atmospheric Research, Boulder, CO, USA, ⁵ARC Centre of Excellence for Climate Extremes, Monash University, Melbourne, VIC, Australia

Abstract The response of precipitation extremes (PEs) to global warming is found to be nonlinear in Community Earth System Model version 1 (CESM1) and other global climate models (Pendergrass et al., 2019), which led to the concern that it is not accurate to approximate the response of PE to a single forcing as the difference between simulations with all forcing agents and those that exclude one specific forcing. This calls into question previous model-based results that the sensitivity of PE with warming due to aerosol forcing is significantly larger than that due to greenhouse gases (GHGs). We reevaluate the PE sensitivity to GHGs and aerosols using available CESM1 ensemble simulations. We show that although the PE response to warming is nonlinear in CESM1, especially for the high warming projected in the twenty-first-century, PE sensitivity to aerosols is still significantly stronger than that due to GHGs when the comparison is made within similar warming regimes to avoid the bias induced by the nonlinear behavior. But the difference is smaller than previously estimated. We also conclude that the additivity assumption is largely valid to isolate the PE response due to aerosol forcing from the paired simulations including the “all forcing” experiment when the warming regime is small (e.g., 1°C–2°C in the next few decades when aerosol forcing is projected to decline and becomes a major source of uncertainty for model projection).

1. Introduction

How the precipitation extreme (PE), such as the strict metric of the annual maximum daily precipitation (RX-1day_Annual), responds to the past and future climate change is an important question that can inform future regional climate adaptation (Nie et al., 2020; Pfahl et al., 2017; Senéviratne et al., 2021). The “hydrological” sensitivity of PEs to global mean surface temperature (GMST) (dPE/dGMST, expressed as mm/year/°C or in the relative term of %/°C) is a useful indicator for climate model evaluation and climate change projection assessment. Despite being a simple global mean metric, dPE/dGMST is based on a similar rationale behind the well-used quantity of climate sensitivity (as the ratio of GMST to global mean radiative forcing). The identified PE sensitivity can be dependent on precipitation metrics used (Lin et al., 2016) and regions considered (X. Wang, Jiang, & Lang, 2017; Z. Wang, Lin, et al., 2017). In practice, dPE/dGMST is usually obtained by (a) conducting a linear regression using the temperature and PE during a transient warming period or (b) calculating the epoch difference between a warmer and a colder period (Thackeray et al., 2018; Zhao et al., 2018). Both approaches implicitly assume the linearity of PE response to global warming.

The linear assumption was the subject of a recent investigation by Pendergrass et al. (2019), which showed that in the full suite of CMIP5-class models, CESM1 and a few others demonstrate a strong nonlinearity in terms of PE and GMST relationship. The nonlinearity features a positive high-order term when fitting PE and GMST using a quadratic function, which means the slope of dPE/dGMST (i.e., PE sensitivity) becomes larger in warmer regimes, regardless of the forcing agents leading to the warmer temperature. Although the exact mechanisms behind the nonlinear behaviors remain unclear, it is shown that the tropical ocean PE has the largest nonlinearity, while the mid-latitude PE over land, important for hydroclimate and flooding, appears to be largely linear (Table

Writing – review & editing: Yangyang Xu, Zhili Wang, Julie Arblaster

S1 of Pendergrass et al., 2019). Note that the nonlinearity of PE response can also be dependent on the climate models and precipitation metrics.

The main implication of the nonlinear behavior in the CESM1, if indeed a valid representation of the real world, is that the future PE increase would be even larger than projections based on unweighted multi-model mean results because a fraction of models does not exhibit a strong nonlinear behavior. The underestimation is potentially large when the global warming goes beyond 3°C (relative to the preindustrial era) toward the second half of this century, a pathway likely under medium to high-emission scenarios.

Regarding the near-term warming (e.g., a further 1°C projected for the first half of this century), the nonlinearity appears to be weak according to the previous study, so the underestimation of projected PE increase using the multi-model mean framework might not be severe in the near-term. But there is another layer of complexity. The warming in the next few decades can be enhanced by aerosols. Aerosol cooling will likely be quickly reversed or even eliminated in the next few decades due to clean-air regulation in developing nations, thus will impose a positive forcing on the climate system relative to the present-day (Lelieveld et al., 2019; X. Wang, Jiang, & Lang, 2017; Z. Wang et al., 2016; Z. Wang, Lin, et al., 2017), likely to introduce warming that is more regionally confined than GHG warming.

Our previous CESM1-based analysis suggested that $dPE/dGMST$ is larger in response to aerosols than GHGs (Lin et al., 2016). If such a conclusion is robust, it has a major implication for anticipating future PE changes. That is, the projected PE increase in the near-term (up to mid twenty-first-century), forced by both an incremental GHG increase and a drastic decrease in aerosol forcing, can be even stronger than the long-term projection (toward the end of twenty-first-century) mostly driven by GHG forcing. The upcoming stronger near-term change pose great burden for adaptation at vulnerable regions.

Because of the identified nonlinearity behavior (notably in CESM1), Pendergrass et al. (2019) raised doubts that the GHG/aerosol partitioning procedure in Lin et al. (2016), using a paired set of twenty-first-century CESM1 warming experiments, was biased. Therefore, given the demonstrated nonlinearity in CESM1, it is crucial to revisit the conclusion of Lin et al. (2016) that “the increased rate of PEs with warming caused by aerosol forcing is significantly larger than that caused by GHG forcing”. This motivates us to carry out a comprehensive reexamination of Lin et al. (2016), using several statistical methods and various newly available CESM1 simulations. The generalization of results here to other models is also discussed.

2. Methods

We use a number of large ensemble (LE) simulation from CESM1, which includes three categories (color-coded differently in Table 1):

1. The recently available transient twentieth- and twenty-first-century (1920–2080) single forcing simulations: “FixedGHG1920”, “FixedIndustrialAER1920”, and “FixedBiomassBurningAER1920” (Deser et al., 2020). These are all branched from the CESM1 LE simulation with all forcing included (Kay et al., 2015). FixedGHG1920 means climate simulation with historical (1920–2005) and RCP8.5 (Radiative Concentration Pathways 8.5) (2006–2080) external forcings but constant GHG emissions (i.e., GHG radiation forcing 0.63 W/m²). FixedIndustrialAER1920 simulated with fixed industrial aerosols emissions at 1920 conditions while all other external forcings evolve follow historical (1920–2005) and RCP8.5 (2006–2080) scenarios
2. The twenty-first-century only (2006–2100) simulation that has GHG and aerosol forcing separately fixed: “FixedAER2005” and “FixedGHG2005” FixedAER2005 is a scenario with constant (non-declining) aerosol emissions after 2005 but with GHG forcing increase as in RCP8.5 (Xu et al., 2015). Conversely, FixedGHG2005 is a scenario with constant (non-increasing) GHG forcing after 2005 but with aerosol declining as in RCP8.5
3. The twentieth-century only (1850–2005) simulation that has GHG and aerosol forcing separately included: “GHG-only” and “AER-only” (per CMIP5 design as in Meehl et al., 2014), or separately excluded: “FixedGHG1850” (GHG radiative forcing fixed at about 0.20 W/m²), “FixedAER1850” (this study)

To the best of our knowledge, we have included all of the available CESM1 experiments that are designed to probe into the role of individual forcing of long-lived GHGs (CO₂, N₂O, CFC/HCFC) and aerosols. (Other individual forcing experiments are also available e.g., ozone, land use, etc. but are not evaluated here due to their

Table 1
Model Experiments

Runs.	35	20	20	15	15	15	2	3	3
Years	1920–2100	1920–2080	1920–2080	1920–2030	2006–2100	2006–2100	1850–2005	1850–2005	1850–2005
Forcing	CMIP5 historical forcing before 2005 and RCP8.5 after 2005. The primary climate response can be calculated by contrast with LE. to GHG and aerosol.	Same as LE but fixing GHG in 1920. The primary climate response to aerosol. The GHG forced response can be calculated by contrast with LE.	Same as LE but fixing Industrial aerosols in 1920. The primary climate response to GHG and the aerosol without the industrial category. The impact of industrial aerosol can be obtained by contrasting this simulation with LE.	Same as LE but fixing Biomass Burning aerosols in 1920. The primary climate response to the aerosol that without biomass burning category.	RCP8.5 but fixing GHG in 2005. The primary climate response to aerosol.	RCP8.5 but fixing aerosols in 2005. The primary climate response to GHG.	CMIP5 historical forcing but with GHG only. The climate response to GHG.	CMIP5 historical forcing but with aerosol only. The climate response to aerosol.	CMIP5 historical forcing except for GHG. The primary climate response to aerosol.
Short names	LE	FixedGHG1920	FixedIndustrialAER1920	FixedBiomassBurningAER1920	FixedGHG2005	FixedAER2005	GHG-only	AER-only	FixedGHG1850 FixedAER1850

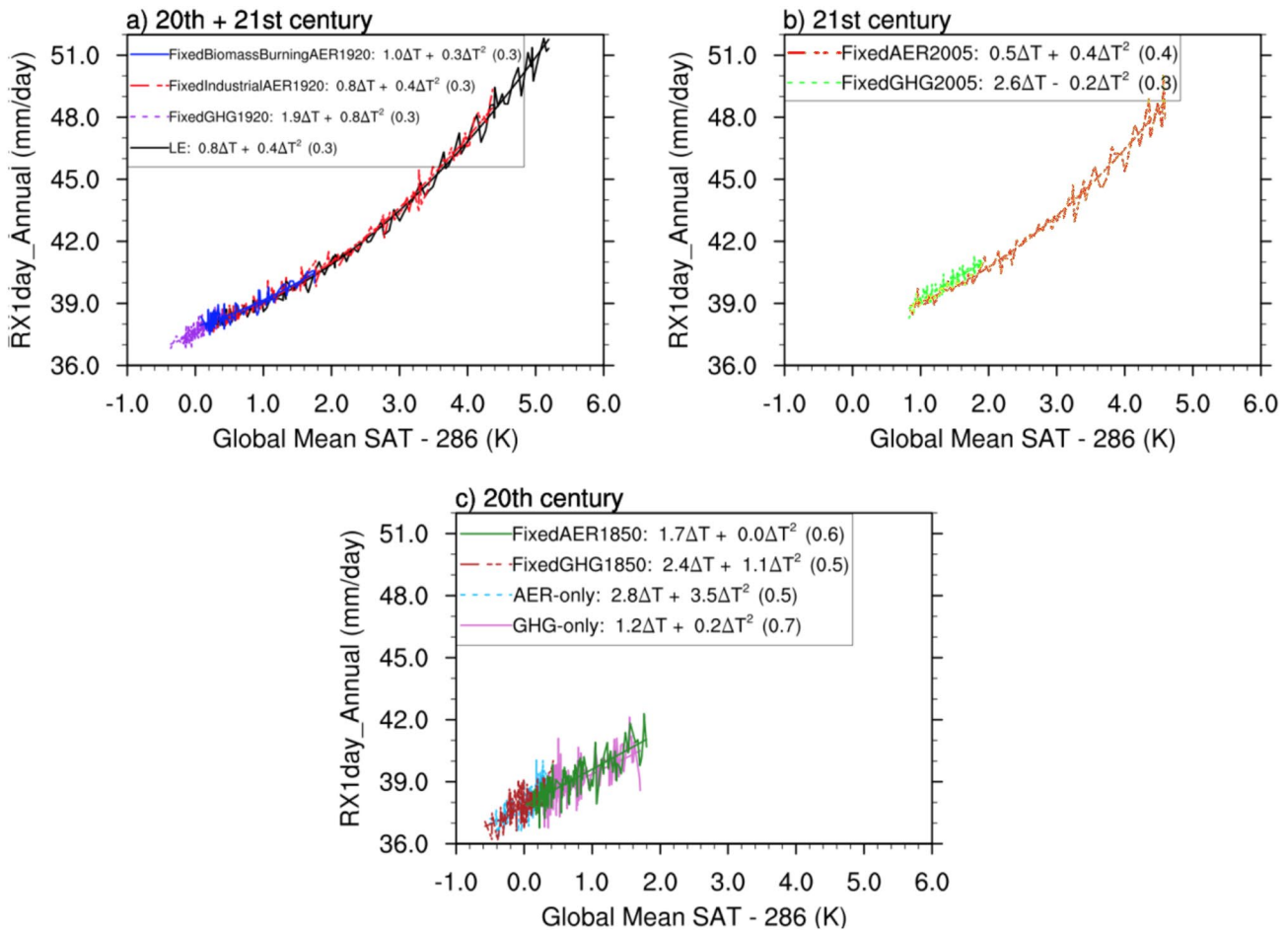


Figure 1. Quadratic polynomial fit of all sets of CESM1 experiment, panel (a) for LE: historical forcing (1920–2005) and RCP8.5 forcing (2006–2100), FixedGHG1920 (1920–2005), FixedIndustrialAER1920 (1920–2005) and FixedBiomassBurning1920 (1920–2005); panel (b) for FixedAER2005 (2006–2100) and FixedGHG2005 (2006–2100); panel (c) for GHG-only (1850–2005), AER-only (1850–2005), FixedGHG1850 (1850–2005) and FixedAER1850 (1850–2005). Only the ensemble average is shown, and thus the smaller ensemble in (c) shows larger fluctuation. The x-axis is the global mean surface air temperature (shown as an anomaly relative to 286K). The y-axis is the global mean RX1day_Annual in mm/day (absolute values). The values in parentheses in the legend are the root mean squared error (RMSE) of the fitted curves. Note that a smaller RMSE indicates a closer fit.

weaker climate response at a global scale.) These include single forcing experiments per CMIP5 protocol, and also post-CMIP5 activities using the “all-but-one” or “leave-one-out” approaches. CESM1 contribution to this aspect appears to be the most comprehensive one among all CMIP5 models. Note that many experiments used here feature a LE (>10 members), enabling a more robust PE sampling and uncertainty quantification. The evolution of PE as a function of temperature from all the experiments is shown in Figure 1 for reference.

3. Robust PE Response to Global Forcing: Addressing the Issues of Linearity and Additivity

Before we get into the question of GHG and aerosol relative sensitivity in influencing PE, we first address the following technical questions:

1. Is the derived PE response ($dPE/dGMST$) sensitive to the methods adopted?
2. Is the PE change at different levels of global warming linear?
3. Is the PE response to different forcings additive?

We first test the robustness of four different approaches to obtain the PE sensitivity, namely using linear regression with decadal average, using linear regression with the annual average, using non-parametric regression

Table 2
dPE/dGMST From Various Methods, All Using the 35-Member LE Experiment in Table 1

LE (%/°C)	Slope using the decadal average over 2010–2040 (the least squared method)	Slope using the annual average over 2010–2040 (the least squared method)	Slope using the annual average over 2010–2040 (Sen's slope)	Epoch difference (2035–2045 – 2005–2015)
Global	4.8 ± 0.6	5.2 ± 0.4	5.3 ± 1.4	4.8 ± 0.6
Global land	6.4 ± 0.2	6.6 ± 0.3	6.5 ± 0.6	6.5 ± 0.7
Global ocean	4.3 ± 0.7	4.8 ± 0.5	4.8 ± 1.4	4.3 ± 0.7
Tropics	4.7 ± 0.7	5.3 ± 0.7	5.3 ± 1.8	4.9 ± 0.9
Mid-latitude (North)	6.0 ± 0.1	6.0 ± 0.2	5.9 ± 0.5	5.7 ± 0.4
Mid-latitude (South)	5.1 ± 0.2	4.9 ± 0.2	4.9 ± 0.4	4.6 ± 0.5

Note. The values after "±" are the uncertainty (as the standard deviation among ensemble members). The linear fit is based on NCAR Command Language's built-in least squared function "regline_stats". Sen's slope is a robust method that is non-sensitive to outliers (Sen, 1968).

(Sen, 1968) with the annual average, and using epoch differences. We only show the results from the LE experiment in the twentieth- and twenty-first-centuries for simplicity. The key point here is that the difference in dPE/dGMST among those methods is statistically indistinguishable and is much smaller than the difference in the PE sensitivity due to aerosol and GHG forcing as later shown. Indeed, the difference in each row of Table 2 is not large enough for individual slope estimates to be statistically different (i.e., unable to pass the *t* test at a 5% confidence level).

The typical method for estimating the slope of a regression line that fits a set of data is based on the least squares estimate, which is not valid when the data elements do not fit a straight line; it is also sensitive to outliers. In addition to the least squared method, the Sen's estimator (Sen, 1968), which does not assume linear slope for all data and is not sensitive to the outlier, was also used to calculate the slope. Sen's slope yields similar results (Table 2).

Second, we confirm there is indeed strong nonlinearity in CESM1 experiments. This is demonstrated in Figure 2 from two perspectives:

1. The nonlinearity in the percentage response of RX1day_Annual to the warming, highlighted by Pendergrass et al. (2019), was confirmed. The linear slope is different between the lower and higher warming regimes. The slope of the first 1.5°C is 4.8%/°C, while the slope of the last 1.5°C (3.5°C–5°C) is more than doubled (9.9%/°C) (Figure 2)
2. The polynomial fit (with the 2nd order) has the quadratic term positive (1.0). The root mean squared errors between the quadratic fit and the linear fit are also smaller (0.8 vs. 2.0), consistent with Pendergrass et al. (2019) who show that CESM1 is one of the models with the largest PE nonlinearity

The nonlinearity in a larger warming range (e.g., 0°C–5°C relative to the Year 1920) as in Figure 2 indicates that in quantifying the relative sensitivity of PE to different forcing agencies (e.g., aerosols vs. GHGs), one should avoid comparing results obtained from different warming regimes. For example, the aerosol-induced PE sensitivity in the 20th-century should not be directly compared with the GHG-induced PE sensitivity in the twenty-first-century.

Figure 2 also shows the year 2000, 2020, ..., 2080 above the *x*-axis to indicate the temperature change at that year, for example, LE projects a 1.8°C increase in GMST at 2040 relative to 1920. We note that the linearity largely holds within a smaller warming range (e.g., the first 1.5°C increase for 2005–2045 in Figure 2), with a small RMSE of the linear fit (0.7) that is on par with the RMSE of the quadratic fit. Therefore, alternatively, one can focus on the same small warming regime (e.g., smaller than 2°C) to quantify the dPE/dGMST. This is a "direct" quantification of PE sensitivity and will be further explored in the next section.

Third, we test whether the additivity of various forcing holds, that is, whether dPE/dGMST in response to "GHGs + aerosols" is the same as dPE/dGMST to "GHGs", plus dPE/dGMST to "aerosols". This is important because the aerosol-induced change has been derived as the difference between all forcing and "everything but aerosols" experiments, in many previous studies (Deser et al., 2020; Ming et al., 2010). Lin et al. (2016) also used the subtraction/differential/residual method to obtain aerosol and GHG-induced responses. More fundamentally, the derived PE sensitivity due to individual forcing is less useful for understanding climate change projection's dependence on atmospheric composition, if the additivity is not valid.

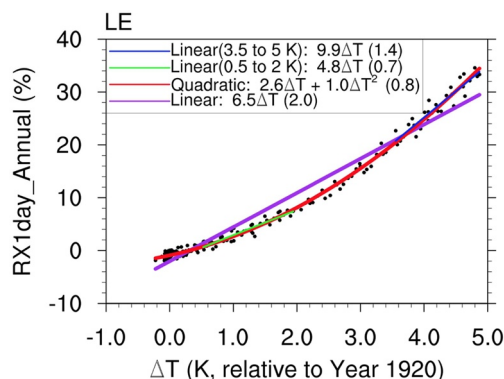


Figure 2. CESM-LE (1920–2100) ensemble-, global-, annual-average of RX1day_Annual (%), relative to 1979–2005 vs. temperature change (K, relative to the year of 1920). The values in parentheses in the legend mean: root mean squared error (RMSE). "Quadratic": Quadratic Polynomial. The red line denotes the quadratic polynomial fitting, while the purple, green and blue line denotes the linear fitting over the whole, 0.5–2.0, and 3.5–5 K temperature change range, respectively. The year added above the *x*-axis shown in vertical font indicates the temperature change that year.

Table 3
PE Sensitivity (%/°C) Due to Aerosols and GHGs

%/°C	20th-century (AER/GHG-only)	20th + 21st-century (LE - FixedIndustrialAER1920/LE - FixedBiomassBurningAER1920/ LE - FixedGHG1920)	21st-century (LE - FixedAER2005/LE - FixedGHG2005)	Same as the 21st-century column, but LE - FixedGHG2005 is based on the high-warming regime (green in Figure 3g)
Global	5.8 ± 0.8/3.8 ± 0.3	4.4 ± 0.6/8.4 ± 1.3/5.6 ± 0.1	14.1 ± 0.8/8.5 ± 0.2	11.9 ± 1.3
Global land	9.7 ± 0.7/5.5 ± 0.4	8.8 ± 0.5/7.1 ± 1.2/6.3 ± 0.1	13.9 ± 0.6/8.0 ± 0.1	9.8 ± 1.0
Global ocean	4.5 ± 0.9/3.2 ± 0.4	3.0 ± 0.8/8.8 ± 1.6/5.4 ± 0.1	14.2 ± 0.9/8.7 ± 0.2	12.6 ± 1.5
Tropics	6.3 ± 1.3/3.1 ± 0.5	4.1 ± 1.0/11.0 ± 2.0/6.0 ± 0.2	19.3 ± 1.2/10.4 ± 0.3	15.5 ± 2.1
Mid-latitude (North)	7.2 ± 0.4/5.3 ± 0.3	7.6 ± 0.3/7.6 ± 0.8/5.2 ± 0.0	10.4 ± 0.3/5.8 ± 0.1	6.3 ± 0.5
Mid-latitude (South)	4.5 ± 0.5/5.4 ± 0.2	3.0 ± 0.4/-0.1 ± 0.8/5.6 ± 0.0	4.3 ± 0.4/6.5 ± 0.1	7.6 ± 0.6

Notes. The values are based on the ensemble average. The values after "±" are the standard error of the estimated linear slopes due to variability within the ensemble. "LE minus Fixed aerosol" represents aerosol responses, while "LE minus Fixed GHG" represents GHG responses.

Using the twentieth-century simulations, we find that the sensitivity due to GHG forcing is $3.8 \pm 0.3\%/^{\circ}\text{C}$ from historical GHG-only run (Table 3), and $4.2 \pm 0.3\%/^{\circ}\text{C}$ from historical all-forcing run minus "all but GHG run (FixedGHG1850)" (not shown in Table 3). The two sensitivities are different but are still statistically indistinguishable at a 95% confidence level (following *t* test). At the same time, the sensitivity to aerosol is $5.8 \pm 0.8\%/^{\circ}\text{C}$ based on historical aerosol forcing only run, and $5.3 \pm 0.5\%/^{\circ}\text{C}$ based on historical forcing run minus "all but excluding the aerosol forcing run (FixedAER1850)" (not shown in Table 3), and again statistically indistinguishable. Thus, at least for the purpose of studying PE sensitivity to warming at a global level, it's safe to assume additivity when using the "all-but-one" approach.

However, we note that the lack of distinction presented above might be because we have only examined the twentieth-century historical period, where the warming is much smaller than in the twenty-first-century, and not large enough to rise above the internal variability of RX1day_Annual . Presumably, the additivity will break down in the twenty-first-century warming regime when the nonlinearity is large, but the lack of the corresponding paired simulation for the twenty-first-century precludes such a direct confirmation.

Lastly, we summarize this section:

1. Because of insensitivity to the method selected, in the following analysis, we will adopt the method of using linear regression of annual average, which is different from Pendergrass et al. (2019) based on the epoch difference method
2. Because of the concern over additivity breakdown, in the next section (GHGs vs. aerosols), we will use two approaches to obtain the relative contribution: one indirectly with subtraction/differentiation/residual, and one directly without subtraction
3. Because of the apparent nonlinearity, when using either approach above, we carefully select the warming regimes over which the sensitivity ($d\text{PE}/d\text{GMST}$) is derived

4. GHGs Vs. Aerosols

We now test the validity of the main conclusion of Lin et al. (2016) that aerosols induce a larger PE response sensitivity than GHGs. In Figure 3, we calculate the PE responses to aerosols vs. GHGs using various CESM1 simulations including the twenty-first-century (Xu et al., 2015), the twentieth-century (Meehl et al., 2013), and the twentieth- and twenty-first-century period (Deser et al., 2020). Overall, we find that the aerosols (see Section 4.1 for the discussion on the industrial and biomass burning aerosols) consistently induce a larger sensitivity compared to the GHGs results (right column of Figure 3). The difference between the aerosol-induced sensitivity and GHG-induced sensitivity is always larger than one standard deviation and often two standard deviations.

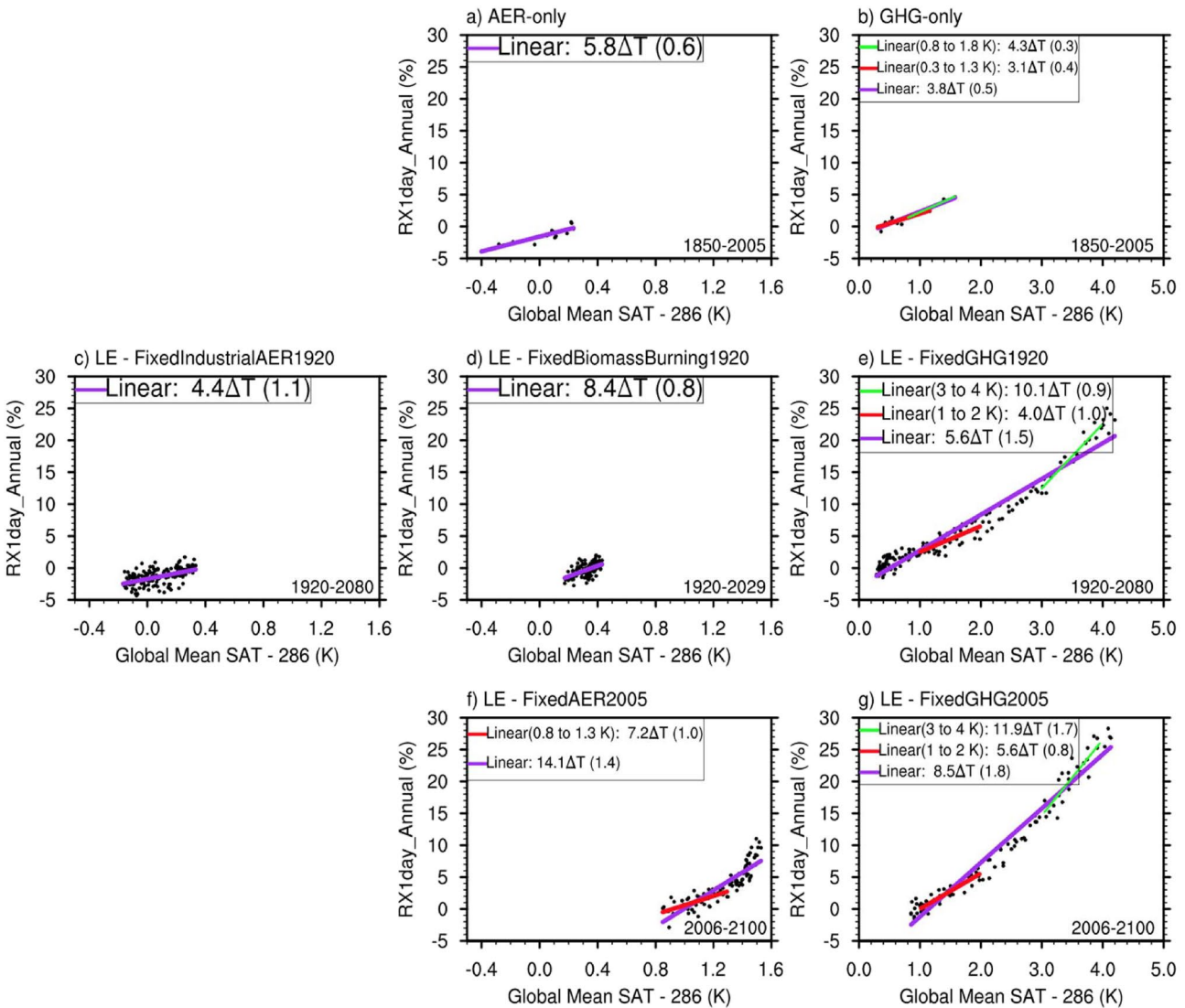


Figure 3. The linear fit to obtain the sensitivity of PE to warming driven by the forcings of aerosols (left columns) and GHGs (rightmost column). The values in parentheses in the legend are root mean squared error. The slopes are summarized in Table 3 including other regional averages. The purple denotes the linear fitting over the entire temperature change range. The green and blue lines denote the linear fit over different smaller warming windows. Global Mean SAT (surface air temperature) from the model runs are subtracted by an arbitrary number of 286 K (about 13°C) to derive the anomaly warming which is relevant to obtaining sensitivity.

However, as explained in Section 3, the nonlinearity will ultimately lead to the breakdown of the additivity. Thus, we next explore the $dPE/dGMST$ in response to GHGs and aerosols using both approaches, one with the subtraction (i.e., the residual method) and one without the subtraction. The advantages and limitations of both approaches are discussed in detail.

4.1. Indirectly Using the Subtraction Approach

In many previous studies, the single forcing effect on climate is isolated using a pair of simulations in which that specific forcing in question is included or not. Using the twentieth- and twenty-first-century simulation (Column 2 of Table 3), the global mean PE response to aerosols is consistently larger than the GHGs, with the difference significantly larger than the uncertainty range. For example, over global land, different category aerosols induce a sensitivity of 7.1–8.8%/°C, while the GHGs only induced a weaker sensitivity of 6.3%/°C.

The exception comes from the industrial aerosol-induced PE changes, where aerosols have a weaker sensitivity than GHGs in the globe (4.4 vs. 5.6%/K), global ocean, and tropics region, and only have a slightly stronger

Table 4
Similar to Table 3 but Expressed as the Ratio of Aerosols Induced Sensitivity Vs. GHG-Induced Sensitivity (Unitless)

	Twentieth-century warming (AA/GHG-only)	Twentieth + twenty-first (based on the simple average of industrial and biomass aerosols in Table 3)	Twenty-first warming (LE - FixedAER2005/LE - FixedGHG2005)	Twenty-first warming (LE - FixedAER2005/LE - FixedGHG2005), but only using the high-warming regime
Global	1.5	1.1	1.7	1.2
Global land	1.8	1.3	1.7	1.4
Global ocean	1.4	1.1	1.6	1.1
Tropics	2.0	1.3	1.9	1.2
Mid-latitude (North)	1.4	1.5	1.8	1.7
Mid-latitude (South)	0.8	0.3	0.7	0.6

sensitivity over global land and NH mid-latitude regions. The reason is aerosol forcing from industrial sectors is primarily from NH mid-latitudes, in contrast to the aerosol forcing from biomass burning sectors primarily from the tropics. Since the mid-latitude aerosols (assuming the magnitude of forcing is similar as in the tropical aerosols) is more capable of inducing a larger global mean temperature response (Shindell & Faluvegi, 2009; Westervelt et al., 2018), but a smaller precipitation change, the PE sensitivity due to those mid-latitude aerosols are smaller than tropical aerosols (almost by half globally, and more than by half over ocean and tropics; Column 2 of Table 3). Indeed, biomass-burning aerosols, in all cases except for SH mid-latitudes, induced a significantly larger sensitivity than GHGs. Furthermore, we find a simple average of the two consistently being larger than the GHG-induced sensitivity (shown as the Aerosol/GHG ratio in Table 4, Column 2).

In Table 4, Aerosol/GHG sensitivity ratios (computed from Table 3) from all three pairs of the simulation are always larger than one over global, global land, global ocean, tropics, and Northern Hemisphere midlatitudes. The Southern Hemisphere mid-latitudes have a less-than-one ratio because of the lack of aerosol emission sources there. The ratio is particularly large in using the 21st-century simulation (as in Lin et al., 2016), which is put into the test next.

One critique from Pendergrass et al. (2019) is that one cannot use the LE minus FixedAER2005 result as the aerosol signal, because that the additional warming is induced by aerosols on top of the GHG warming and is thus subject to the sensitivity enhancement due to the nonlinearity identified in a high warming regime (exceeding 3°C). The nonlinearity of RX1day_Annual inevitably leads to the problem of additivity, especially when the span of underlying warming is large. As a result, the residual method (in this Section 4.1), although widely used in many previous analyses, has its inherent limitation because of additivity assumption, which is likely to break down in the twenty-first-century warming regime (Section 3). Because of the sensitivity enhancement due to nonlinearity, the residual method would tend to overestimate the aerosol-induced sensitivity, while only slightly

overestimate the GHGs response. This is because the bias in each residual estimate due to the nonlinearity is inversely proportional to the temperature response to that forcing. Since aerosols have a smaller temperature response than GHGs, the residual method would exaggerate the response to aerosols more than to GHGs.

Here, we examine this critique by comparing the aerosol and GHG signals but only using GHG response within a higher warming regime (3.5–5 K, the blue line in Figure 2). During this high warming regime, understandably, the GHG-induced sensitivity is also larger. For example, comparing the third and the fourth column of Table 3, 8.5 vs. 11.9%/K for the global average. We note that, even when adopting the larger GHG sensitivity, the aerosol/GHG ratio becomes smaller but remains consistently greater than 1 (Table 4, Column 4). Table 5 is the same as Table 4 but for three different periods (near future, mid-twenty-first century, and end of the twenty-first century), which clearly

Table 5
Similar to Table 3 but Expressed as the Ratio of Aerosols to GHGs Sensitivity (Unitless) for Different Periods

LE - FixedAER2005/LE - FixedGHG2005	2020–2060	2040–2080	2060–2100
Global	2.0	2.2	3.0
Global land	2.0	1.9	1.9
Global ocean	2.0	2.3	3.4
Tropics	2.4	2.6	3.4
Mid-latitude (North)	2.0	1.8	1.5
Mid-latitude (South)	0.5	1.0	1.4

shows that a comparison over the same time period, even if it is not too long and with valid linearity, can be misleading, because the underlying warming can be very different from one case to another.

4.2. Directly Using Model Output

Because of the apparent limitation of the residual method (Section 4.1), we next use single-forcing experiments directly (within a similar warming regime), to answer the question of climate change due to specific forcing.

Using the direct model output of single forcing experiments of the twentieth century in which the linearity is largely held (panel c of Figure 1 and Column 1 of Table 3), the GHGs-induced sensitivity is $3.8 \pm 0.3\%/^{\circ}\text{C}$ compared to $5.8 \pm 0.8\%/^{\circ}\text{C}$ due to aerosols, with the difference significantly larger than the uncertainty range. As indicated by the 1st column of Table 4, this is also consistently true for land and ocean as well as other geographical regions except for SH midlatitude where the aerosol forcing is weak. The ratio of extreme precipitation response to aerosol vs. GHG forcing (Table 4) is also larger over land than the ocean and larger in the NH, all consistent with the expected stronger aerosol forcing over NH land. Thus, based on the 20th-century simulations, we reaffirm the AER/GHG ratio being larger than 1, despite smaller than that obtained in Lin et al. (2016) using the residual methods over the twenty-first-century simulation. The larger-than-one ratio, using the direct approach over twentieth-century simulation, is also previously found for other CMIP5 models (Lin et al., 2018).

Because of the concern that nonlinearity will emerge above the internal variability only in the 21st-century warming regime, we next attempt to repeat the direct approach above but using the twentieth + twenty-first-century simulation (Deser et al., 2020), as well as the twenty-first-century simulation (Xu et al., 2015).

One may propose to directly use FixedIndustrialAER1920 to approximate the response of GHGs and use FixedGHG1920 to approximate the response of aerosols. However, this approach is severely flawed because the volcanic forcing is included in both FixedGHG1920 and FixedIndustrialAER1920 simulations for the 20th-century portion. Since volcanic forcing (via stratospheric aerosols) is distinct from GHGs in terms of causing hydrological responses (Bala et al., 2005; Xu et al., 2020), FixedIndustrialAER1920 is not suitable to mimic the response due to GHGs.

Therefore, the currently available model experiments leave us only one option—using the twenty-first-century single forcing experiment (FixedAER2005 from Xu et al., 2015, and the follow-up FixedGHG2005 runs) to directly infer the response of GHGs and aerosols. However, we carefully only compare the responses within a similar temperature range to minimize the influence of nonlinearity. Had we considered the entire temperature range, it will be easy to come to the wrong conclusion that GHG induced change (purple curves on the left panels of Figure 4) is larger than that due to aerosols (purple curves on the right panels of Figure 4), but because of the uptick of sensitivity due to the apparent nonlinearity.

In Figure 4, just focusing on the red lines where the warming is small (1°C due to the aerosol forcing or just a small fraction of GHG during the first few decades of the 21st-century), the aerosols induced sensitivity (left, FixedGHG2005) is consistently bigger than that due to GHGs (right, FixedAER2005), regardless of whether we do ensemble average, decadal average, or running decadal average (5.1–5.3 vs. 4.3–4.4%/K, range from the top three rows of Figure 4). The difference with a ratio of 1.2, and consistent with the subtraction method (1.2 in Column 4 of Table 4), which also only considered a smaller warming regime. The aerosol/GHG ratio of 1.2 is statistically robust (all of the differences of Figure 4 passing the significance test) but smaller than the ratio based on Lin et al. (2016) method (i.e., 1.7 in Table 4). What is more, we also showed the twenty-first-century portion of FixedIndustrialAER1920 (FixedGHG1920) to approximate the response of GHGs (aerosols) in the last row of Figure 4, that is, the year 2006–2080, since there is no volcanic eruption after 2005. The results are consistent with the twenty-first century single forcing run (i.e., FixedAER2005 and FixedGHG2005, respectively).

5. Conclusions

Using a variety of single forcing ensemble simulations, we confirm that CESM1 PE response indeed has a strong feature of nonlinear response. The debate is then centered around whether the sensitivity of RX1day_Annual ($\%/^{\circ}\text{C}$) is larger in response to aerosol forcing than in response to GHG forcing, as indicated by Lin et al. (2016), or it is an artifact due to the overlooked nonlinearity in the analysis.

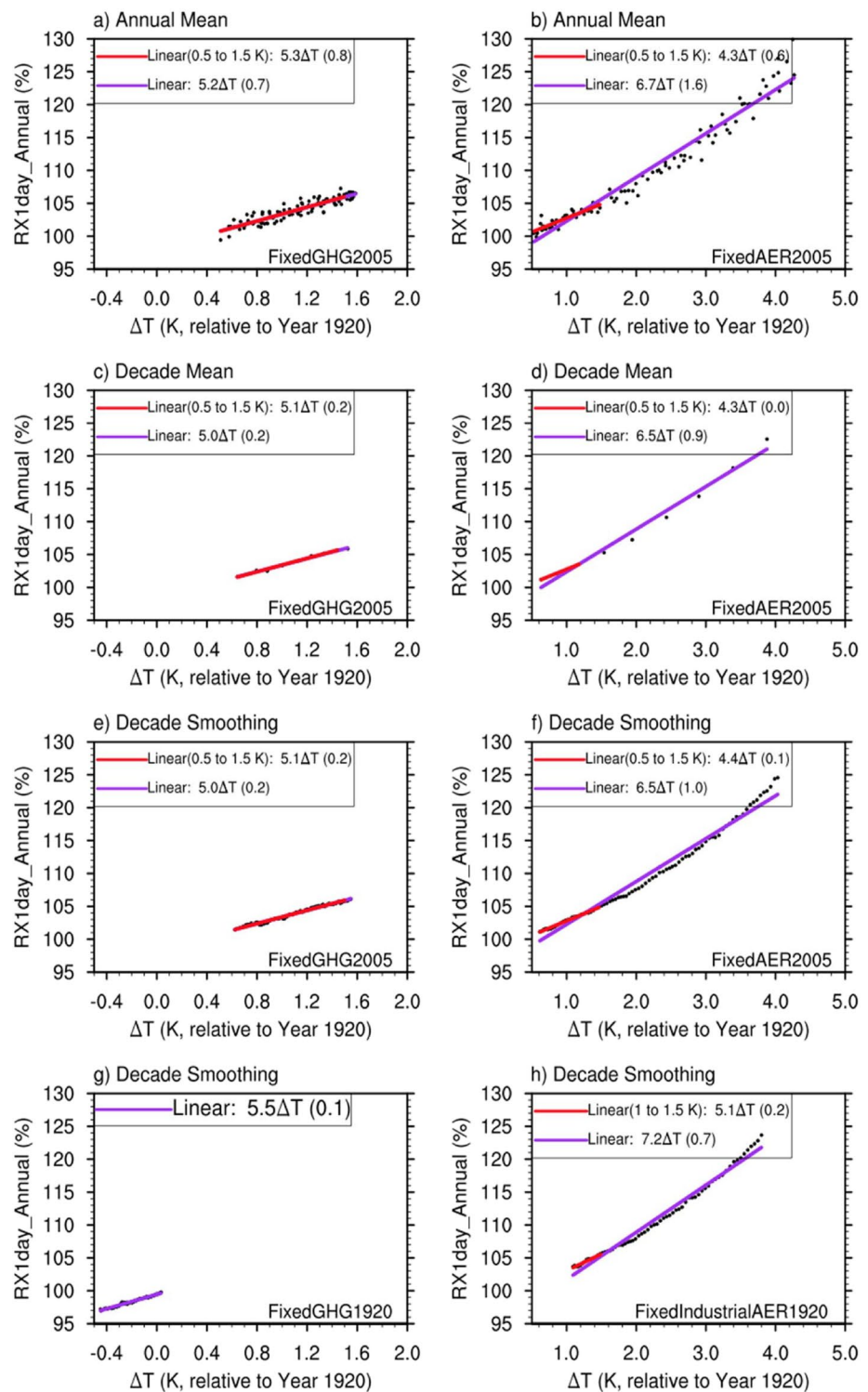


Figure 4. Using the twenty-first-century simulation as it is, without any subtraction to approximate aerosols (left) and GHG (right). Annual mean (95 data points from 2006 to 2100), decadal mean (9 data points from average of (2007–2016), ..., an average of (2017–2026), ..., an average of (2087–2096)) and 10 yr equal-weighted smoothing (95 data points from 2006 to 2100) are shown for the first, second and third row, respectively. The last row showed the twenty-first-century portion of FixedGHG1920 and FixedIndustrial1920 (i.e., 2006–2080) run with 10 yr equal-weighted smoothing. The values in parentheses in the legend are root mean squared error. The purple denotes the linear fitting over the whole temperature change range. The red lines denote the linear fit over different warming windows.

Due to the nonlinearity, it is not straightforward to pin down a specific response of RX1day_Annual to different forcings, because the response to just one forcing can vary depending on what temperature the simulation is at. The easiest way is to look at the direct model output, instead of using the subtraction method, in similar warming regimes (e.g., within 1°C warming range when the linearity largely holds).

First, it is clear that the twentieth-century runs (during which the warming is small, and thus the nonlinearity is small compared to noise) support this argument, and so did other CMIP5 models (Lin et al., 2018). Second, using the 20th-century and the twenty-first-century runs, we show Aerosol/GHG ratio for RX1day_Annual is consistently larger than 1 (1.1–1.7) in CESM1, especially for the global land region and NH mid-latitudes (Table 4). Note, however, the results here are smaller than the reported ratio of 2–in Lin et al. (2016) but closer to Lin et al. (2018) where other CMIP5 models are considered (the ratio for RX1day is founded to be 1.4 in the multi-model ensemble). It is also worth noting that even for a high GHG emission scenario like RCP8.5, the simulated global warming is rather limited until after 2050. Therefore, the identified nonlinearity in CESM1 would be not very important in the next few decades.

The physical argument of a stronger PE sensitivity to aerosols than GHG stems from the fast response of precipitation to atmospheric adjustment. The CO₂ increase induces an atmospheric positive forcing which lead to inhibiting effects on precipitation increase initially (Myhre et al., 2018; Samset et al., 2016), which is later overwhelmed by the surface warming effects (Samset et al., 2018). This inhibiting effect of fast adjustment is missing in response to majority of aerosols (dominated by SO₂ which has weak absorption). While this contrast between GHG and aerosols is most evident for mean precipitation response, the effect is still noticeable for other PE metrics including RX1day (Lin et al., 2018; Sillmann et al., 2019).

Previous analysis in PDRMIP (Precipitation Driver Response Model Intercomparison Project) assuming much stronger idealized single forcing, yielded consistent result as the CESM1 twentieth-century single forcing run, highlighting the role of fast adjustment (Sillmann et al., 2019). Because of the lack of fixed SST experiments here, we are not able to quantitatively probe into the contribution of rapid adjustment process due to aerosols and due to GHGs. However, the stronger PE sensitivity due to aerosol forcing as comprehensively demonstrated here and shown in our previous study based on the CMIP5 twentieth-century historical multimodel simulations (Lin et al., 2018) suggest the key role of fast adjustment, consistent with previous PDRMIP related studies.

For future research, when the single forcing LE simulations from CESM2 or other CMIP6 models (see Li et al., 2021) become available, one could revisit this problem (especially the contrasts between industrial and biomass burning related aerosols), because CESM2 has an even stronger aerosol forcing (Gettelman et al., 2019), but a weaker nonlinearity (1.0%/°C² for CESM1, 0.4%/°C² for CESM2; Pendergrass et al., 2019). This can be done in conjunction with CCSM4, an older version prior to CESM1, which had a smaller aerosol forcing (due to the lack of consideration of aerosol indirect effects) but a similar nonlinearity.

Data Availability Statement

The CESM1 Large Ensemble simulation in Kay et al. (2015) can be found at <http://www.cesm.ucar.edu/projects/community-projects/LENS/data-sets.html>. The transient twentieth- and twenty-first-century (1920–2080) single forcing simulations in Deser et al. (2020) can be found at http://www.cesm.ucar.edu/working_groups/CVC/simulations/cesm1-single_forcing_le.html. The twenty-first century only (2006–2100) simulation that has GHG and aerosol forcing separately fixed in Xu et al. (2015) can be found at <https://www.cgd.ucar.edu/projects/chsp/brace-output-projections.html>. The twentieth century only (1850–2005) simulation that has GHG and aerosol forcing separately included in Meehl et al. (2013) can be found at <https://esgf-node.llnl.gov/search/cmip5/>. The twentieth century only (1850–2005) simulation that has GHG and aerosol forcing separately excluded are archived at https://portal.neresc.gov/archive/home/c/ccsm/www/Lei_Yangyang_etal.

References

- Arblaster, J. M., & Meehl, G. A. (2006). Contributions of external forcings to southern annular mode trends. *Journal of Climate*, 19(12), 2896–2905. <https://doi.org/10.1175/JCLI3774.1>
- Bala, G., Caldeira, K., Mirin, A., Wickett, M., & Delire, C. (2005). Multicentury changes to the global climate and carbon cycle: Results from a coupled climate and carbon cycle model. *Journal of Climate*, 18(21), 4531–4544. <https://doi.org/10.1175/JCLI3542.1>

Acknowledgments

We acknowledge helpful discussions with Dr. Angie Pendergrass. The TAMU team thanks support from the US National Science Foundation (Climate and Large-scale Dynamics Program; AGS-1841308). ZW is supported by the National Natural Science Foundation of China (41875179). JA acknowledges support from the Australian Research Council Centre of Excellence for Climate Extremes (Grant CE170100023) and the U.S. Department of Energy, Office of Science, Office of Biological & Environmental Research (BER), Regional and Global Model Analysis (RGMA) component of the Earth and Environmental System Modeling Program under Award Number DE-SC0022070. This research used resources of the National Energy Research Scientific Computing Center (NERSC), a U.S. Department of Energy Office of Science User Facility located at Lawrence Berkeley National Laboratory, operated under Contract No. DE-AC02-05CH11231. This research also used resources of Computational and Information Systems Laboratory in National Center for Atmospheric Research. The National Center for Atmospheric Research (NCAR) is a major facility sponsored by the NSF under Cooperative Agreement No. 1852977.

- Deser, C., Phillips, A. S., Simpson, I. R., Rosenbloom, N., Coleman, D., Lehner, F., et al. (2020). Isolating the evolving contributions of anthropogenic aerosols and greenhouse gases: A new CESM1 large ensemble community resource. *Journal of Climate*, 33(18), 7835–7858. <https://doi.org/10.1175/JCLI-D-20-0123.1>
- Gottelman, A., Hannay, C., Bacmeister, J. T., Neale, R. B., Pendergrass, A. G., Danabasoglu, G., et al. (2019). High climate sensitivity in the Community Earth System Model Version 2 (CESM2). *Geophysical Research Letters*, 46, 8329–8337. <https://doi.org/10.1029/2019GL083978>
- Kay, J. E., Deser, C., Phillips, A., Mai, A., Hannay, C., & Strand, G., et al. (2015). The Community Earth System Model (CESM) large ensemble project: A community resource for studying climate change in the presence of internal climate variability. *Bulletin of the American Meteorological Society*, 1333–1349. <https://doi.org/10.1175/BAMS-D-13-00255.1>
- Lelieveld, J., Klingmüller, K., Pozzer, A., Burnett, R. T., Haines, A., & Ramanathan, V. (2019). Effects of fossil fuel and total anthropogenic emission removal on public health and climate. *Proceedings of the National Academy of Sciences*, 116(15), 7192–7197. <https://doi.org/10.1073/pnas.1819989116>
- Li, C., Zwiers, F., Zhang, X., Li, G., Sun, Y., Wehner, M. (2021). Changes in annual extremes of daily temperature and precipitation in CMIP6 models. *Journal of Climate*, 34(9), 3441–3460. <https://doi.org/10.1175/jcli-d-19-1013.1>
- Liguori, G., McGregor, S., Arblaster, J. M., Singh, M. S., & Meehl, G. A. (2020). A joint role for forced and internally driven variability in the decadal modulation of global warming. *Nature Communications*, 11, 3827. <https://doi.org/10.1038/s41467-020-17683-7>
- Lin, L., Wang, Z., Xu, Y., & Fu, Q. (2016). Sensitivity of precipitation extremes to radiative forcing of greenhouse gases and aerosols. *Geophysical Research Letters*, 43(18), 9860–9868. <https://doi.org/10.1002/2016GL070869>
- Lin, L., Xu, Y., Wang, Z., Diao, C., Dong, W., & Xie, S.-P. (2018). Changes in extreme rainfall over India and China attributed to regional aerosol-cloud interaction during the late 20th-century rapid industrialization. *Geophysical Research Letters*, 45(15), 7857–7865. <https://doi.org/10.1029/2018gl078308>
- Meehl, G. A., Washington, W. M., Arblaster, J. M., Hu, A., Teng, H., Kay, J. E., et al. (2013). Climate change projections in CESM1(CAM5) compared to CCSM4. *Journal of Climate*, 26(17), 6287–6308.
- Ming, Y., Ramaswamy, V., & Persad, G. (2010). Two opposing effects of absorbing aerosols on global-mean precipitation. *Geophysical Research Letters*, 37(13). <https://doi.org/10.1029/2010GL042895>
- Mortier, A., Gliss, J., Schulz, M., Aas, W., Andrews, E., Bian, H., et al. (2020). Evaluation of climate model aerosol trends with ground-based observations over the last two decades—An AeroCom and CMIP6 analysis. *Atmospheric Chemistry and Physics*, 20(21), 13355–13378. <https://doi.org/10.5194/acp-20-13355-2020>
- Myhre, G., Kramer, R. J., Smith, C. J., Hodnebrog, Ø., Forster, P., Soden, B. J., et al. (2018). Quantifying the importance of rapid adjustments for global precipitation changes. *Geophysical Research Letters*, 45(20), 11399–11405. <https://doi.org/10.1029/2018GL079474>
- Nie, J., Dai, P., & Sobel, A. H. (2020). Dry and moist dynamics shape regional patterns of extreme precipitation sensitivity. *Proceedings of the National Academy of Sciences*, 117(16), 8757–8763. <https://doi.org/10.1073/pnas.1913584117>
- Pendergrass, A. G., Coleman, D. B., Deser, C., Lehner, F., Rosenbloom, N., & Simpson, I. R. (2019). Nonlinear response of extreme precipitation to warming in CESM1. *Geophysical Research Letters*, 46(17–18), 10551–10560. <https://doi.org/10.1029/2019GL084826>
- Pfahl, S., O’Gorman, P. A., & Fischer, E. M. (2017). Understanding the regional pattern of projected future changes in extreme precipitation. *Nature Climate Change*, 7(6), 423–427. <https://doi.org/10.1038/nclimate3287>
- Samset, B. H., Myhre, G., Forster, P. M., Hodnebrog, Ø., Andrews, T., Boucher, O., et al. (2018). Weak hydrological sensitivity to temperature change over land, independent of climate forcing. *npj Climate and Atmospheric Science*, 1, 20173. <https://doi.org/10.1038/s41612-017-0005-5>
- Samset, B. H., Myhre, G., Forster, P. M., Hodnebrog, Ø., Andrews, T., Faluvegi, G., et al. (2016). Fast and slow precipitation responses to individual climate forcings: A PDRMIP multimodel study. *Geophysical Research Letters*, 43(6), 2782–2791. <https://doi.org/10.1002/2016GL068064>
- Sen, P. K. (1968). Estimates of the regression coefficient based on Kendall’s Tau. *Journal of the American Statistical Association*, 63(324), 1379–1389. <https://doi.org/10.1080/01621459.1968.10480934>
- Seneviratne, S. I., Zhang, X., Adnan, M., Badi, W., Dereczynski, A., Di Luca, A., et al. (2021). Weather and climate extreme events in a changing climate. In V. MassonDelmotte, P. Zhai, A. Pirani, S. L. Connors, C. Pean, S. Berger, et al. (Eds.), *Climate change 2021: The physical science basis. Contribution of Working Group I to the Sixth Assessment Report of the Intergovernmental Panel on Climate Change*. Cambridge University Press. In Press.
- Shindell, D. & Faluvegi, G. (2009). Climate response to regional radiative forcing during the 20th-century. *Nature Geoscience*, 2(4), 294–300. <https://doi.org/10.1038/ngeo473>
- Sillmann, J., Stjern, C. W., Myhre, G., Samset, B. H., Hodnebrog, Ø., Andrews, T., et al. (2019). Extreme wet and dry conditions affected differently by greenhouse gases and aerosols. *npj Climate and Atmospheric Science*, 2, 24. <https://doi.org/10.1038/s41612-019-0079-3>
- Thackeray, C. W., DeAngelis, A. M., Hall, A., Swain, D. L., & Qu, X. (2018). On the connection between global hydrologic sensitivity and regional wet extremes. *Geophysical Research Letters*, 45(20), 11343–11351. <https://doi.org/10.1029/2018GL079698>
- Wang, X., Jiang, D., & Lang, X. (2017). Future extreme climate changes linked to global warming intensity. *Science Bulletin*, 62, 1673–1680.
- Wang, Z., Lin, L., Yang, M., Xu, Y. (2016). The effect of future reduction in aerosol emissions on climate extremes in China. *Climate Dynamics*, 47 (9–10), 2885–2899. <https://doi.org/10.1007/s00382-016-3003-0>
- Wang, Z., Lin, L., Zhang, X., Zhang, H., Liu, L., & Xu, Y. (2017). Scenario dependence of future changes in climate extremes under 1.5°C and 2°C global warming. *Scientific Reports*, 7(1), 1–9. <https://doi.org/10.1038/srep46432>
- Westervelt, D. M., Conley, A. J., Fiore, A. M., Lamarque, J.-F., Shindell, D. T., Previdi, M., et al. (2018). Connecting regional aerosol emissions reductions to local and remote precipitation responses. *Atmospheric Chemistry and Physics*, 18, 12461–12475. <https://doi.org/10.5194/acp-18-12461-2018>
- Xu, Y., Lamarque, J. F., & Sanderson, B. M. (2015). The importance of aerosol scenarios in projections of future heat extremes. *Climatic Change*, 146(3), 393–406. <https://doi.org/10.1007/s10584-015-1565-1>
- Xu, Y., Lin, L., Tilmes, S., Dagon, K., Xia, L., Diao, C., et al. (2020). Climate engineering to mitigate the projected 21st-century terrestrial drying of the Americas: A direct comparison of carbon capture and sulfur injection. *Earth System Dynamics*, 11(3), 673–695. <https://doi.org/10.5194/esd-11-673-2020>
- Zhao, A. D., Stevenson, D. S., & Bollasina, M. A. (2018). The role of anthropogenic aerosols in future precipitation extremes over the Asian Monsoon Region. *Climate Dynamics*, 52, 6257–6278. <https://doi.org/10.1007/s00382-018-4514-7>